# Epitope-specific antibody response is controlled by immunoglobulin $V_H$ polymorphisms

Bruno Raposo,[1] Doreen Dobritzsch,[2] Changrong Ge,[1] Diana Ekman,[1] Bingze Xu,[1] Ingrid Lindh,[1] Michael Förster,[1] Hüseyin Uysal,[1] Kutty Selva Nandakumar,[1] Gunter Schneider,[2] and Rikard Holmdahl[1]

[1]Section for Medical Inflammation Research and [2]Section for Molecular Structural Biology, Department of Medical Biochemistry and Biophysics, Karolinska Institutet, 171 77 Stockholm, Sweden

**Autoantibody formation is essential for the development of certain autoimmune diseases like rheumatoid arthritis (RA). Anti-type II collagen (CII) antibodies are found in RA patients; they interact with cartilage in vivo and are often highly pathogenic in the mouse. Autoreactivity to CII is directed to multiple epitopes and conserved between mice and humans. We have previously mapped the antibody response to CII in a heterogeneous stock cohort of mice, with a strong association with the *IgH* locus. We positioned the genetic polymorphisms and determined the structural requirements controlling antibody recognition of one of the major CII epitopes. Polymorphisms at positions S31R and W33T of the associated variable heavy chain ($V_H$) allele were identified and confirmed by gene sequencing. The Fab fragment binding the J1 epitope was crystallized, and site-directed mutagenesis confirmed the importance of those two variants for antigen recognition. Back mutation to germline sequence provided evidence for a preexisting recognition of the J1 epitope. These data demonstrate a genetic association of epitope-specific antibody responses with specific $V_H$ alleles, and it highlights the importance of germline-encoded antibodies in the pathogenesis of antibody-mediated autoimmune diseases.**

CORRESPONDENCE
Rikard Holmdahl:
Rikard.Holmdahl@ki.se

Abbreviations used: CII, type II collagen; CDR, complementarity-determining region; CIA, collagen-induced arthritis; HS, heterogeneous stock; RA, rheumatoid arthritis; ScFv, single chain fragment variable; SPR, surface plasmon resonance; $V_H$, variable heavy chain; $V_L$, variable light chain.

The way pathogenic autoantibodies escape immune tolerance is a key feature for the understanding of autoimmune diseases. The production of autoantibodies such as rheumatoid factors or anti-citrullinated protein antibodies constitutes a hallmark in the diagnosis of rheumatoid arthritis (RA; Aletaha et al., 2010). Type II collagen (CII) is the main protein constituent of articular and hyaline cartilage, and autoantibodies to CII develop around the clinical onset of arthritis (Fujii et al., 1992; Mullazehi et al., 2007). Immunization of mice with CII induces an inflammatory polyarthritis (collagen-induced arthritis [CIA]), mimicking major features of human RA (Brand et al., 2007). The B cell response to CII plays an important role in the development of the disease (Svensson et al., 1998; Luross and Williams, 2001). The passive transfer of arthritis to naive mice by anti-CII reactive serum (Stuart and Dixon, 1983; Holmdahl et al., 1990) or specific anti-CII mAb (Holmdahl et al., 1986; Nandakumar et al., 2003) demonstrates the pathogenicity of such antibodies in mediating inflammation of the joints. Among the mAbs recognizing CII structures, those binding to the epitopes C1, U1, and J1 have been shown to be arthritogenic (Bajtner et al., 2005), whereas the CII-F4 antibody recognizing the F4 epitope is protective (Burkhardt et al., 2002). The mAb M2139 specifically recognizes the J1 epitope (Karlsson et al., 1995) and is the most arthritogenic anti-CII mAb in the mouse, eliciting disease upon single transfer (Nandakumar and Holmdahl, 2005). Autoreactivity to CII is evolutionary conserved between mice and humans. Reactive B cells to the same CII epitopes as those described in CIA have been identified in humans (Burkhardt et al., 2002), thus strengthening the role of this animal model to study the production and reactivity of autoantibodies toward CII.

In this study, we define the genetic association of autoantibody production during arthritis

D. Dobritzsch's present address is Section of Biochemstry, Department of Chemistry – BMC, Uppsala University, 171 23 Uppsala, Sweden.



The Rockefeller University Press $30.00
J. Exp. Med. 2014 Vol. 211 No. 3 405-411
www.jem.org/cgi/doi/10.1084/jem.20130968

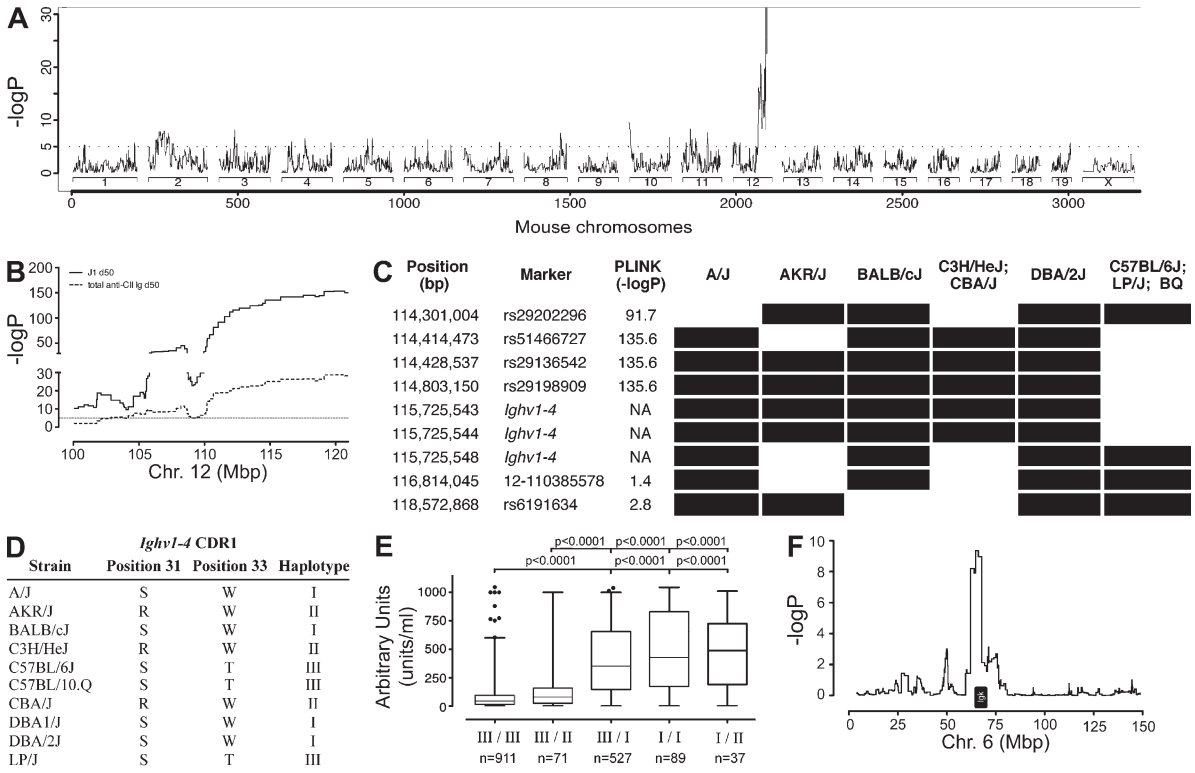


**Figure 1. Genes in the IgH locus control autoreactive anti-J1 antibody response.** (A) Genome-wide association of the anti-J1 antibody production maps to the *IgH* locus on chromosome 12. Only approximately one fifth of the scale is represented. (B) Zoom-in of the *IgH* association observed in A and comparison to the association obtained for total anti-CII Ig response in the same locus. P-values were obtained using the haplotype reconstruction method HAPPY ($n$ = 1,640). (C) Haplotype reconstruction of the *IgH* locus surrounding the *Ighv1-4* gene. Black bars indicate an identical allele to the reference DBA/1J strain. PLINK obtained p-values. (D) Grouping of the reference and HS cohort strains in relation to the allele variants observed in the *Ighv1-4* CDR1. (E) Anti-J1 antibody titers stratified by different HS strains and their *IgH* haplotype. P-values were calculated by Mann-Whitney test. Error bars indicate the 1–99th percentile, with the dark circles representing the outliers within each haplotype. (F) Mapping of the kappa locus on chromosome 6 indicated by 22 BQ-haplotype mice (III) showing high titers of anti-J1 antibodies in E. P-values were determined by HAPPY using a binary phenotype (anti-J1 titers higher or lower than 400 AU).

development. The structural and molecular interactions observed in the $M2139_{Fab}$–J1 immune complex demonstrate the importance of germline-encoded sequences for peptide recognition. These data indicate that epitope-specific antibody responses recognized by germline-encoded structures are of significant relevance for the development of autoantibody-mediated autoimmune diseases.

## RESULTS AND DISCUSSION

### A single gene in the Ig variable heavy chain ($V_H$) locus governs the anti-J1 antibody response

Antibodies to the triple helical J1 epitope of CII are arthritogenic and constitute one of the pathogenic factors in CIA (Mo and Holmdahl, 1996; Bajtner et al., 2005). To determine the genetic contribution to this specific antibody response, we analyzed plasma samples from a previously described heterogeneous stock (HS) cohort (Ahlqvist et al., 2011; Förster et al., 2012). The nearly unique genome-wide association was mapped to the *Ig heavy chain* (*IgH*) locus on chromosome 12, with a −logP = 156.3 (Fig. 1, A and B). Previously, different genetic elements in the *IgH* locus were found to be associated with the development of RA (Olee et al., 1991; Vencovský et al., 2002) and multiple sclerosis (Buck et al., 2013). However, these associations have been postulated using candidate gene approaches, or generally mapped to the overall production of antibodies with disregard for the involved antigen. The lack of genome-wide associations in human autoimmune diseases mapping to the *IgH* locus may be accounted for by the allelic and copy number variations in the region, as well as by the variability of $V_H$ gene usage between individuals (Glanville et al., 2011). To our knowledge, this is the first study evidencing a genome-wide association to the *IgH* locus with the production of specific antibody reactivity. Interestingly, this finding concerns pathogenic autoantibodies recognizing a well-characterized autoantigen.

To pinpoint the genes responsible for this association in the mouse, we resequenced all the existing and previously identified anti-J1 mAbs (Mo and Holmdahl, 1996) by capillary sequencing. It turns out that these are all somatically mutated mAbs with different rearranged variable light chains ($V_L$s) but sharing the same $V_H$ allele, encoded by the *Ighv1-4* gene (Ensembl Mouse, NCBI m37 assembly). Based on the HS

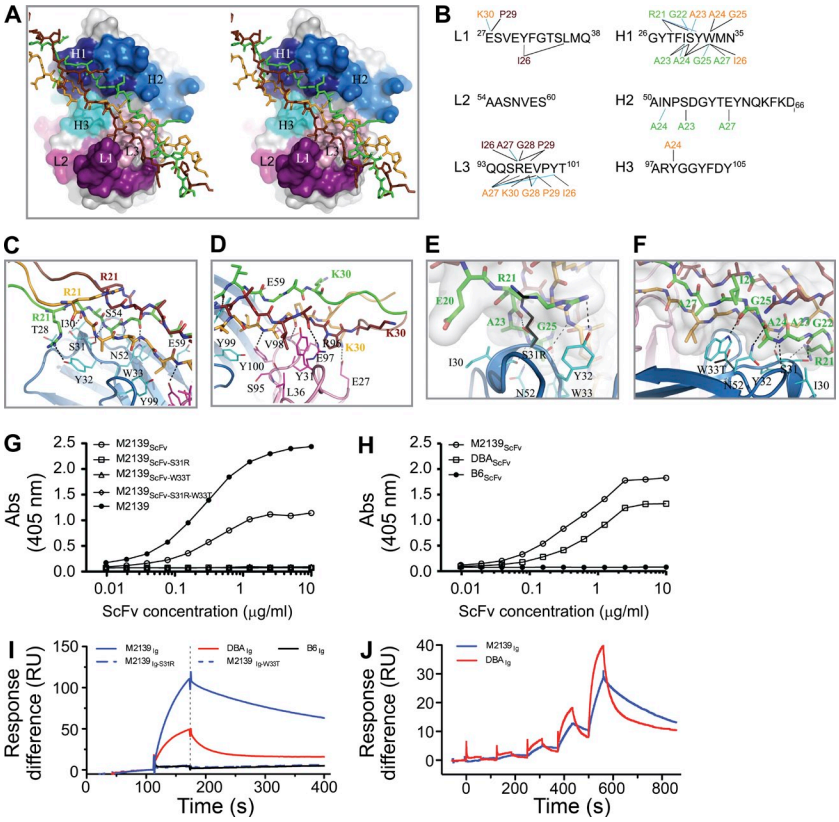


**Figure 2. Crystal structure of the M2139$_{Fab}$–J1 complex and $V_H$ CDR1 polymorphisms.** (A) Stereo view cartoon representation of the epitope–paratope interface. The Fab is represented as gray solid surfaces except for the CDR regions, which are labeled and colored in blue shades for the heavy chain and pink/purple for the light chain. The triple-helical J1 peptide chains are shown as sticks in green, orange, and brown. (B) Schematic view of the contacts between residues of the hypervariable region of the M2139$_{Fab}$ and the J1 peptide. The variable domains are classified using the Kabat numbering system. Above and below the CDR sequences, the interacting residues of the triple-helical J1 peptide are listed. Hydrogen bonds and salt bridges are depicted in blue lines, and hydrophobic and van der Waals contacts as black lines. The peptide residues are shown in green, brown, and orange when belonging to the E, F, and G strands, respectively, and numbered according to their position in the synthetic peptide. (C and D) Representation of the major Fab-peptide contacts in the M2139$_{Fab}$–J1 complex. The triple helical peptide is presented in green, orange, and brown, whereas the Fab heavy chain is presented in blue and the light chain in pink. (E and F) View of the mutation sites S31R and W33T in the M2139$_{Fab}$, respectively. The variable domains of the Fab are shown in blue cartoon representations. J1 peptide residues are depicted with carbon atoms in the same colors as described in A, with nitrogen atoms in blue and oxygen atoms in red. J1 residues are numbered according to their sequence in the synthetic peptide. Heavy chain residues interacting with the J1 epitope are depicted with carbon atoms in cyan, whereas the arginine and threonine side chains occurring at the variable sites 31 and 33 of the heavy chain CDR1 are shown with black carbon atoms. Hydrogen bonds are represented as dotted lines. (G and H) Recognition of the triple-helical J1 peptide by the M2139 ScFv variants (G) and by the respective DBA/1J (DBA$_{ScFv}$) and C57BL/6J (B6$_{ScFv}$) germline sequences (H). Data are representative of three independent experiments. (I and J) Association and dissociation curves from the M2139-derived full recombinant Igs by SPR (vertical dashed line separates the association and dissociation phases of the antibodies with the J1 peptide; I), and the respective thermodynamic and kinetic parameters for M2139$_{Ig}$ and DBA$_{Ig}$ (J), using single-cycle kinetics. Data are representative of two independent experiments.

founder strains, we reconstructed the haplotype of the locus surrounding the identified $V_H$ allele. We identified three different haplotypes occurring in our HS cohort (Fig. 1 C): I, II, and III (Fig. 1 D). Whereas the mouse strains from haplotype I—A/J, BALB/cJ, and DBA/2J—share the highest similarity with the reference strain DBA/1J, the mouse strains carrying haplotype III—C57BL/6J, C57BL/10.Q (BQ), and LP/J—present the most distinctive alleles. Moreover, two major variants in the complementarity-determining region 1 (CDR1) of the associated $V_H$ allele were found: a serine-to-arginine substitution at position 31 (S31R; haplotype II presented by AKR/J, C3H/HeJ, and CBA/J) and a tryptophan-to-threonine exchange at position 33 (W33T, haplotype III; Fig. 1 D). We thus stratified the anti-J1 antibody response in accordance with the observed haplotypes. This demonstrated that the great majority of mice with either a type II or III haplotype were not able to mount a proper anti-J1 response, whereas a single copy of the haplotype I resulted in a very significant increase of anti-J1 titers (Fig. 1 E). Yet, a small percentage of mice with haplotype III (22 out of 911) produced anti-J1 antibodies in a relatively high amount (>400 arbitrary units [AU]). Hence, we hypothesized that a different genetic regulation, though possibly similar within these 22 animals, could be responsible for the elevated anti-J1 titers. A new genetic analysis revealed that the *Igκ* locus on chromosome 6 was associated with the phenotype although not with genome-wide significance (Fig. 1 F).

### Crystallization, structure determination, and overall structure of the M2139$_{Fab}$–J1

To determine the relevance of the identified polymorphisms to the overall structural recognition of the J1 epitope, we crystallized the M2139 mAb Fab fragment in complex with the triple-helical form of the J1 epitope (M2139$_{Fab}$–J1 complex). The M2139$_{Fab}$–J1 crystallized in space group $P3_121$ with one complex per asymmetric unit (Table S1). The structure was determined to a resolution of 3.25 Å by molecular replacement, with observation of continuous electron density for residues 1–216 of both heavy (H) and light (L) chains. For the triple-helical J1 peptide, electron density was observed for residues 11–35, 10–34, and 9–34 of the leading (chain E), middle (chain G), and trailing (chain F) strands, respectively. The M2139$_{Fab}$ shows the canonical Fab fragment domain

organization and fold, with each of the Ig domains containing an intramolecular disulfide bridge (L:23-L:92, L:138-L:198, H:22-H:96, and H:143-H:198). Likewise, the J1 peptide provided evidence for the typical CII triple-helical conformation (Bella et al., 1994), with hydrogen bonding between the amide groups of the glycine residues of the repeated Gly-X-Y motifs and backbone carbonyl groups from adjacent chains. The R21 residues from all three chains stabilize this network further by side chain–mediated hydrogen bonds.

The interface formed between $M2139_{Fab}$–J1 covers an area of ∼840 Å$^2$, corresponding to ∼17 and 4% of the solvent-accessible surface areas of the peptide and Fab, respectively. All but one (L2) of the CDR loops is in contact with the peptide, with CDRs H1 and L3 being the main contributors to the interface area (Fig. 2, A and B; and Tables S2 and S3). Contacts are made primarily to the middle and leading strands of the peptide, as they penetrate deepest into the peptide-binding cleft (Fig. 2, A, C, and D). The trailing strand mostly faces away from the Fab but can be reached by the protruding CDRs of the light chain. From the 15 residues of the J1 epitope, all but the first two are recognized by the $M2139_{Fab}$ in at least one of the peptide chains, with the $I_{26}A_{27}G_{28}$ triplet of each peptide chain being in contact with the Fab residues (Table S3). In contrast, none of the G-P-O repeats used for stabilizing the triple helical structure of the J1 peptide is contacted by Fab residues. The complex formation is dominated by hydrophobic and van der Waals interactions but also involves nine hydrogen bonds and two salt bridges (Table S4). The $M2139_{Fab}$–J1 complex superimposes remarkably well with our previously described crystal structure of the collagen C1 epitope bound to the Fab fragment of the CIIC1 antibody ($CIIC1_{Fab}$-C1; Dobritzsch et al., 2011). However, whereas the triple helix of the C1 peptide lies relatively straight in the binding groove of the $CIIC1_{Fab}$, the J1 peptide is slightly bent into the peptide groove of the $M2139_{Fab}$ and crosses it at a different angle (not depicted). The sequences of the hypervariable regions of both Fabs are relatively well conserved. Due to the periodic occurrence of glycine residues and the presence of the *R-G-hydrophobic* motif, the two collagen peptides also show a certain similarity to each other. It would thus be reasonable to expect that several crucial interactions for recognition of triple-helical collagen-like peptides by RA-associated antibodies are conserved. However, this is not the case because a hydrogen bond between the backbone amide of residue 98 of the light chain (L:V98 in $M2139_{Fab}$; and L:D98 in $CIIC1_{Fab}$) and a carbonyl group of the peptide (G:G28 in J1; and G:T21 in C1) is the only feature shared by these complexes (not depicted).

### Peptide binding and $V_H$ CDR1 sequence dependency

With the crystal structure of the $M2139_{Fab}$–J1 complex as a template, we modeled the amino acid polymorphisms found in the CDR1 domain, S31R and W33T (Fig. 2, E and F). We observed that these amino acid residues are major contributors to the $M2139_{Fab}$–J1 affinity interactions (Table S2), and both modifications result in a significant alteration of the contacts between the Fab and the J1 peptide. Both S31 and W33 form hydrogen bonds with G22 and G25 of strand E, respectively. Moreover, they both largely contribute to van der Waals, hydrophobic, or polar interactions. When replaced, S31R and W33T polymorphisms abolish the hydrogen bonding and most other interactions. In addition, the presence of an arginine at position 31 would cause serious steric clashes and thus prevent formation of a Fab–peptide complex with the same geometry as observed in the crystal structure. Thus, either of the amino acid replacements is expected to result in a much weaker binding of the peptide.

To challenge our hypothesis, several single chain fragment variables (ScFv's) were produced, coding for the M2139 sequence ($M2139_{ScFv}$) as well as each of the identified polymorphisms ($M2139_{ScFv\text{-}S31R}$, $M2139_{ScFv\text{-}W33T}$, and $M2139_{ScFv\text{-}S31R\text{-}W33T}$; Fig. S1). As shown in Fig. 2 G, both the $M2139_{ScFv}$ and the full length M2139 antibody are able to bind the triple helical J1 peptide. However, the single amino acid substitutions introduced in the other two variants ($M2139_{ScFv\text{-}S31R}$ and $M2139_{ScFv\text{-}W33T}$) completely abolished the J1 epitope recognition. Similarly, mutation on amino acid R21 of the J1 peptide, which directly interacts with S31 of the $V_H$ domain, was previously shown to abrogate M2139 mAb binding (Burkhardt et al., 2002). Furthermore, we evaluated the J1 recognition by ScFv constructs encoding the *Ighv1-4* germline sequence from either the DBA/1J ($DBA_{ScFv}$) or C57BL/6J ($B6_{ScFv}$) mouse strains. Whereas the $B6_{ScFv}$ was not able to recognize the J1 epitope, the $DBA_{ScFv}$ bound the J1 epitope with a similar but lower strength as compared with the $M2139_{ScFv}$ (Fig. 2 H). To overcome potential issues with the avidity and affinity of the germline-encoded sequences, we produced full recombinant mouse IgG2b antibodies encoding each of the germline sequences ($DBA_{Ig}$ and $B6_{Ig}$) as well as the identified single mutant versions of the M2139 antibody (Figs. S1 and S2). Similarly to the ScFv, only the recombinant $DBA_{Ig}$ germline sequence recognized the J1 epitope of CII. The surface plasmon resonance (SPR) assay (Fig. 2, I and J) clearly showed that the somatically mutated M2139 antibody constitutes a much stronger binder ($K_D$ = 3.88E$^{-8}$ M; $k_{on}$ = 6.89E$^4$ Ms$^{-1}$; $k_{off}$ = 0.002676 s$^{-1}$) than its germline-encoded sequence ($K_D$ = 2.74E$^{-7}$ M; $k_{on}$ = 1.63E$^4$ Ms$^{-1}$; $k_{off}$ = 0.004456 s$^{-1}$). Although clearly binding its epitope, the $DBA_{Ig}$–J1 recognition was found to fit a two-state model, rather than a 1:1 fit as with the $M2139_{Ig}$–J1 complex. This suggests that the $DBA_{Ig}$–J1 occurs with a conformational change of the antibody, in a fairly dynamic way. Nevertheless, our data strongly indicates that the production of J1-specific autoantibodies is germline encoded, and the somatic mutations observed in the M2139 antibody (Fig. S1) occur in an already autoreactive germline-encoded $V_H$ sequence. Together with the strong MHC dependency observed for the CIA mouse model (Wooley et al., 1981; Brunsberg et al., 1994; Nandakumar et al., 2011), our data suggests that the Ig loci of different mouse strains also control the autoantibody response.

### Concluding remarks

The strong genetic control of anti-J1 CII epitope response by a specific $V_H$ allele can be explained if the germline-encoded

$V_H$ genes in the locus dominate such response. Although all of the known J1-specific antibodies contain various amino acid variations due to somatic mutations, they all use a conserved $V_H$ allele. The crystal structure of such allele could show that the interactions with the antigen are dependent on germline-encoded structures and not on the somatically mutated residues. Another example of germline-encoded specificity regards the C1 epitope of CII (Mo and Holmdahl, 1996; Dobritzsch et al., 2011). These antibodies are also autoreactive and pathogenic, and it has been shown that even if the selected V(D)J sequence is expressed as a knockin fragment, the produced germline antibodies do not develop somatic mutations, nor are they negatively selected despite their potential pathogenicity (Cao et al., 2011). Being a T cell–dependent response, it is striking that the antibody response to the autoantigen CII is $V_H$-associated to several of its epitopes (Förster et al., 2012), clearly indicating that the response to CII is largely germline encoded. The requirement for a germline-encoded response could explain why a $V_H$ genetic association has so far not been described. As the CII response is truly autoreactive, and anti-CII antibodies bind their target in vivo and are largely pathogenic, these data are likely to be of importance for the understanding of the role of autoantibodies in autoimmune diseases.

## MATERIALS AND METHODS

**Animals used and CIA induction.** The animals used for CIA have been previously described (Ahlqvist et al., 2011). Briefly, the HS mice derived from the Northport stock comprise eight inbred mouse strains: A/J, AKR/J, BALB/cJ, C3H/HeJ, C57BL/6J, CBA/J, DBA/2J, and LP/J. To rend HS mice susceptible to CIA (Klaczkowska et al., 2011), HS mice were backcrossed in an F3 intercross with C57BL/10.Q. From the resulting offspring, mice expressing the arthritis-permissive MHC class II allele $A^q$ ($n$ = 1,764) were selected for the experiment. Mice were immunized with 100 µg rat CII emulsified in 50 µl CFA, containing 25 µg *Mycobacterium butyricum* (Difco) at day 0, and followed for arthritis development during 50 d. The local ethics committee approved all the animal experiments performed (Lund, Malmö, Sweden: M107-07).

**Anti-J1 epitope ELISA.** All animals used for CIA were bled on days 14 and 50 after immunization from the retro-orbital venous sinus and whole blood was collected in heparinized tubes (10 U/ml). After centrifugation, the resulting plasma was separated and kept at −20°C until assayed. A total of 1,640 samples at each time point were assayed for anti-J1 titers. MaxiSorp plates (Thermo Fisher Scientific) were coated overnight with 5 µg/ml of a triple-helical J1 peptide in PBS at 4°C. After blockage with 2% BSA in PBS, plasma samples were diluted according to a previously determined dilution, and incubated overnight at 4°C. The antibody titers were assessed using HRP-conjugated anti-κ–specific antibody (clone 187.1; SouthernBiotech) and ABTS (Roche) as substrate. The response readout was performed at 405 nm on a Synergy-2 (BioTek Instruments) and an internal standard was used in all ELISA plates to allow comparison of samples between plates.

**HS analysis and statistical inferences.** The data analysis regarding anti-J1 ELISAs has been previously described in detail (Ahlqvist et al., 2011; Förster et al., 2012). In brief, for single locus mapping, the haplotype structure was deduced using the haplotype reconstruction method HAPPY. The threshold of genome-wide significance was considered to be 5% and determined by 200 permutations of the dataset. Age, sex, and batch were used as covariates. To account for the sample structure in the mapping association analysis and minimize the risk of obtaining false positive results, we used a resampling method, generating resample-based model of inclusion probabilities (RMIPs). Single marker associations were performed with PLINK and, alternatively, EMMAX software.

**Ig$V_H$ gene sequencing.** Genomic DNA from the HS-comprised mouse strains and DBA/1J strain was obtained from The Jackson Laboratory, whereas C57BL/10.Q DNA was obtained from our in-house colony. Strain-specific primers amplifying the *Ighv1-4* gene-flanking region of ∼1,000 and 600 bp (first and second PCR products, respectively) were designed for a nested PCR approach. From the first PCR reaction, a single DNA band was purified from 2% agarose gel and used as template for the second PCR reaction. Similarly, the second PCR product was purified and sequenced. Sequencing was performed using BigDye Terminator sequencing kit in a 3730 DNA Analyzer (Applied Biosystems).

**Crystallization and data collection.** Crystals of the M2139 Fab fragment in complex with a triple-helical peptide containing the J1 epitope ($M2139_{Fab}$–J1) were obtained using hanging drop vapor diffusion at 20°C against a reservoir solution containing 1.7 M ammonium sulfate, 0.1 M Hepes, pH 7.5, and 10% (vol/vol) dioxane. The 2 µl drops consisted of equal volumes of protein solution (10 mg/ml $M2139_{Fab}$–J1 in 40 mM Tris, pH 7.5, and 20 mM NaCl) and reservoir solution. Before data collection, the crystals were transferred to reservoir solution supplemented with 25% (vol/vol) glycerol for cryoprotection and immediately thereafter snap-frozen in liquid nitrogen. Crystallographic data were collected at 100 K and a wavelength of 0.975 Å at beamline ID14-EH4 of the European Synchrotron Radiation Facility (Grenoble, France). Data were indexed and integrated using iMOSFLM (Leslie and Powell, 2007) and scaled with SCALA from the CCP4 suite of programs (Collaborative Computational Project, Number 4, 1994). Data collection statistics are given in Table S1.

**Structure determination and refinement.** The crystal structure of $M2139_{Fab}$–J1 was determined by molecular replacement using the program PHASER and the structure of antigen-free $CIIC1_{Fab}$ (Protein Data Bank [PDB] accession number 2y5t; Dobritzsch et al., 2011) as a search model. Density for a triple-helical J1 peptide bound to the Fab was clearly visible in the initial electron density map. Iterations of manual model building in the molecular graphics application COOT were alternated with restrained parameter refinement in REFMAC5. 5% randomly selected reflections were used for monitoring $R_{free}$. No solvent molecules were modeled. PROCHECK (Laskowski et al., 1993) documented 94.8 and 0.4% of the residues in the most favored and disallowed regions of the Ramachandran plot, respectively. Molecular surfaces were analyzed with the Protein Interfaces, Surfaces and Assemblies Service (PISA) at the European Bioinformatics Institute. Crystal structure–related figures were prepared using PyMol. The crystallographic data and structure of the $M2139_{Fab}$–J1 peptide complex have been deposited at PDB with the accession number 4BKL. All software used for acquisition and analysis of crystallographic data have been described elsewhere (Dobritzsch et al., 2011).

**Production and analysis of Fab ScFv and full recombinant Igs.** The amino acid sequence of the antibody fragment, comprising a $V_L$, a synthetic $(G_4S)_4$ linker, and a $V_H$ with C-terminal His-tag (used in ScFv production), as well as the amino acid sequence from the recombinant Igs, are provided in Figs. S1 and S2. The encoding DNA sequence of both the ScFv and full recombinant Igs was synthesized by commercial gene synthesis (EurofinsMWG). For ScFv, the DNA sequence was inserted into the pET-22b expression vector (Novagen) using NcoI and NotI restriction sites to be in frame with the PelB periplasmic secretion signal peptide, whereas for the recombinant Igs the DNA sequence was inserted in the pEX-K vector containing the restriction sites XhoI and XbaI at 5′ and 3′, respectively. The DNA sequence integrity of all constructs was confirmed by DNA sequencing. Amino acid replacements in both ScFv and recombinant Igs were performed by PCR-based site-directed mutagenesis using PFU polymerase (Promega). The mutations were confirmed by DNA sequencing. For expression, all ScFv constructs were separately transformed into *E. coli* BLR (DE3) expression cells. Carbenicillin-containing LB medium was used for initial bacteria inoculation. The resulting bacterial

suspension was transferred into carbenicillin-containing terrific broth (TB) medium and cultured at 37°C. The cultures were induced with 0.5 mM IPTG. For purification, the bacteria cell pellet was lysed and the resulting supernatants containing the ScFv fragments were purified by immobilized metal ion affinity chromatography using Dynabeads, according to the supplier's instructions (Invitrogen). For the recombinant Igs, DH5α cells were used for transformation in kanamycin-containing agar plates. Vectors containing either the light or heavy chain coding DNA were digested with the above-mentioned restriction enzymes and ligated to the mammalian expression vector pCI-neo (Promega) using T4 DNA ligase (Thermo Fisher Scientific). Similarly to the ScFv constructs, the light chain sequence of the M2139 mAb was used in all recombinant Igs, as well as its Ig isotype mouse IgG2b. The new vectors were then transformed into DH5α-competent cells and incubated in LB medium with carbenicillin. Sequence of the transformed vectors was confirmed by DNA sequencing and recombinant vectors were transfected into HEK293T cells. Transfection was obtained by mixing 50 µg of each plasmid containing the light and heavy chain in 1 ml Opti-MEM I (Gibco), followed by mixing with 150 µl lipofectamine 2000 transfection reagent (Invitrogen). After 5 d culture in 10% Ultra-low IgG fetal bovine serum containing DMEM, the recombinant antibodies were purified using a HiTrap protein G HP column (GE Healthcare). A NuPAGE Bis-Tris precast gel (Invitrogen) was used for analysis of the protein samples.

Similarly to the method described above regarding the serologic determination of anti-J1 antibodies, recognition of the J1 epitope by the different ScFv and recombinant Igs was done by ELISA. The response read-out was obtained using an anti-His HRP-conjugated or anti–mouse IgG2b HRP-conjugated antibody, followed by addition of ABTS as enzymatic substrate.

**SPR determination.** The interaction of all five ScFv's with the triple helical J1 peptide was assessed by SPR using a Biacore T200 biosensor (GE Healthcare) at 25°C. J1 peptide was directly covalently coupled to a CM5 sensor chip by amine coupling according to the manufacturer's instructions. An additional flow cell without J1 peptide coupling was used as a blank control. For analysis of the recombinant full length Igs binding the J1 epitope, we used an anti–mouse IgG antibody (GE Healthcare) for capture. In brief, the anti–mouse IgG antibody was coupled covalently to the carboxymethylated dextran of a CM5 sensor chip by amino coupling. $M2139_{Ig}$ and its variants were diluted in PBS-P buffer (20 mM phosphate buffer, 2.7 mM KCl, 137 mM NaCl, and 0.05% Surfactant P20) and injected into the chip at 10 µl/min with a final concentration of 10 µg/ml, to achieve a capture level of ∼1,000 RU. The J1 peptide (10 µg/ml) was then injected over the sensor chip surface for 60 s at a flow rate of 30 µl/min, followed by a 300-s dissociation phase. A regeneration solution (glycine-HCl, pH = 1.7) was used before each run to remove all previously bound molecules. The thermodynamic ($K_D$) and kinetic ($k_{on}$ and $k_{off}$) parameters of the $M2139_{Ig}$ variants binding J1 were determined by single-cycle kinetics. The assay was performed in a continuous flow of 5 µl/min in PBS-P buffer, using five different concentrations of the J1 peptide: (1) 200 nM plus four successive dilutions of one third of the previous concentration for $M2139_{Ig}$ kinetics; and (2) 900 nM plus four successive dilutions of one third of the previous concentration for $DBA_{Ig}$ kinetics. The binding responses were recorded continuously in RU at a frequency of 1 Hz (sensorgrams) and presented as a function of time. Sensorgrams were processed using an automatic correction for nonspecific bulk-refractive-index effects. Data processing and analysis were performed using Biacore T200 evaluation software in a 1:1 binding model (GE Healthcare).

**Sequencing of hybridoma $V_H$.** Total RNA from anti-J1 hybridomas was isolated using PureLink RNA Mini kit (Ambion). $V_H$ sequence of the hybridomas was obtained by SMARTer RACE cDNA amplification kit (Takara Bio Inc.), using RNA as template and primers specific to each Ig constant domain. BigDye Terminator sequencing kit (Applied Biosystems) was used for sequencing of the cDNA products.

**Online supplemental material.** Fig. S1 shows amino acid sequences of the anti-J1 recognizing $V_H$ segments. Fig. S2 shows amino acid sequences of the M2139 antibodies. Table S1 shows $M2139_{Fab}$–J1 crystal data collection and refinement statistics. Table S2 shows CDR contributions to the surface area buried upon interaction of $M2139_{Fab}$ and J1 peptide. Table S3 shows peptide chain contributions to the surface area buried upon interaction of $M2139_{Fab}$ and J1 peptide. Table S4 shows hydrogen bonds between J1 peptide and $M2139_{Fab}$ observed in the $M2139_{Fab}$–J1 complex. Online supplemental material is available at http://www.jem.org/cgi/content/full/jem.20130968/DC1.

We would like to thank Dr. Emma Ahlqvist and Dr. Johan Bäcklund for their critical review of the manuscript, Susanne van den Berg for help with protein purification, and Carlos Palestro and Kristina Palestro for the exceptional animal care. We would also like to thank the GE Healthcare DemoLab at the Science for Life Laboratory (SciLifeLab) Stockholm for technical support in the SPR assays. We also acknowledge the access to synchrotron radiation and helpful support by the beamline staff at the European Synchrotron Radiation Facility (Grenoble, France).

The work was supported by the KA Wallenberg Foundation, the Swedish Research Council, the Swedish Strategic Foundation (SSF), and the EU projects Masterswitch (HEALTH-F2-2008-223404) and EU IMI project BeTheCure. B. Raposo was supported by the Fundação para a Ciência e Tecnologia grant SFRH/BD/40658/2007.

Rikard Holmdahl discloses that he is a co-inventor on a patent protecting the use of CII epitopes for diagnostic use.

**Submitted: 10 May 2013**
**Accepted: 16 January 2014**

## REFERENCES

Ahlqvist, E., D. Ekman, T. Lindvall, M. Popovic, M. Förster, M. Hultqvist, D. Klaczkowska, I. Teneva, M. Johannesson, J. Flint, et al. 2011. High-resolution mapping of a complex disease, a model for rheumatoid arthritis, using heterogeneous stock mice. *Hum. Mol. Genet.* 20:3031–3041. http://dx.doi.org/10.1093/hmg/ddr206

Aletaha, D., T. Neogi, A.J. Silman, J. Funovits, D.T. Felson, C.O.I. Bingham III, N.S. Birnbaum, G.R. Burmester, V.P. Bykerk, M.D. Cohen, et al. 2010. 2010 rheumatoid arthritis classification criteria: an American College of Rheumatology/European League Against Rheumatism collaborative initiative. *Ann. Rheum. Dis.* 69:1580–1588. http://dx.doi.org/10.1136/ard.2010.138461

Bajtner, E., K.S. Nandakumar, Å. Engström, and R. Holmdahl. 2005. Chronic development of collagen-induced arthritis is associated with arthritogenic antibodies against specific epitopes on type II collagen. *Arthritis Res. Ther.* 7:R1148–R1157. http://dx.doi.org/10.1186/ar1800

Bella, J., M. Eaton, B. Brodsky, and H.M. Berman. 1994. Crystal and molecular structure of a collagen-like peptide at 1.9 A resolution. *Science.* 266:75–81. http://dx.doi.org/10.1126/science.7695699

Brand, D.D., K.A. Latham, and E.F. Rosloniec. 2007. Collagen-induced arthritis. *Nat. Protoc.* 2:1269–1275. http://dx.doi.org/10.1038/nprot.2007.173

Brunsberg, U., K. Gustafsson, L. Jansson, E. Michaëlsson, L. Ahrlund-Richter, S. Pettersson, R. Mattsson, and R. Holmdahl. 1994. Expression of a transgenic class II Ab gene confers susceptibility to collagen-induced arthritis. *Eur. J. Immunol.* 24:1698–1702. http://dx.doi.org/10.1002/eji.1830240736

Buck, D., E. Albrecht, M. Aslam, A. Goris, N. Hauenstein, A. Jochim, S. Cepok, V. Grummel, B. Dubois, A. Berthele, et al. Wellcome Trust Case Control Consortium. 2013. Genetic variants in the immunoglobulin heavy chain locus are associated with the IgG index in multiple sclerosis. *Ann. Neurol.* 73:86–94. http://dx.doi.org/10.1002/ana.23749

Burkhardt, H., T. Koller, Å. Engström, K.S. Nandakumar, J. Turnay, H.G. Kraetsch, J.R. Kalden, and R. Holmdahl. 2002. Epitope-specific recognition of type II collagen by rheumatoid arthritis antibodies is shared with recognition by antibodies that are arthritogenic in collagen-induced arthritis in the mouse. *Arthritis Rheum.* 46:2339–2348. http://dx.doi.org/10.1002/art.10472

Cao, D., Ia. Khmaladze, H. Jia, E. Bajtner, K.S. Nandakumar, T. Blom, J.A. Mo, and R. Holmdahl. 2011. Pathogenic autoreactive B cells are not negatively selected toward matrix protein collagen II. *J. Immunol.* 187:4451–4458. http://dx.doi.org/10.4049/jimmunol.1101378

Collaborative Computational Project, Number 4. 1994. The CCP4 suite: programs for protein crystallography. *Acta Crystallogr. D Biol. Crystallogr.* 50:760–763. http://dx.doi.org/10.1107/S0907444994003112

Dobritzsch, D., I. Lindh, H. Uysal, K.S. Nandakumar, H. Burkhardt, G. Schneider, and R. Holmdahl. 2011. Crystal structure of an arthritogenic anticollagen immune complex. *Arthritis Rheum.* 63:3740–3748. http://dx.doi.org/10.1002/art.30611

Förster, M., B. Raposo, D. Ekman, D. Klaczkowska, M. Popovic, K.S. Nandakumar, T. Lindvall, M. Hultqvist, I. Teneva, M. Johannesson, et al. 2012. Genetic control of antibody production during collagen-induced arthritis development in heterogeneous stock mice. *Arthritis Rheum.* 64: 3594–3603. http://dx.doi.org/10.1002/art.34658

Fujii, K., M. Tsuji, A. Kitamura, and K. Murota. 1992. The diagnostic significance of anti-type II collagen antibody assay in rheumatoid arthritis. *Int. Orthop.* 16:272–276. http://dx.doi.org/10.1007/BF00182710

Glanville, J., T.C. Kuo, H.-C. von Büdingen, L. Guey, J. Berka, P.D. Sundar, G. Huerta, G.R. Mehta, J.R. Oksenberg, S.L. Hauser, et al. 2011. Naive antibody gene-segment frequencies are heritable and unaltered by chronic lymphocyte ablation. *Proc. Natl. Acad. Sci. USA.* 108: 20066–20071. http://dx.doi.org/10.1073/pnas.1107498108

Holmdahl, R., K. Rubin, L. Klareskog, E. Larsson, and H. Wigzell. 1986. Characterization of the antibody response in mice with type II collagen-induced arthritis, using monoclonal anti-type II collagen antibodies. *Arthritis Rheum.* 29:400–410. http://dx.doi.org/10.1002/art.1780290314

Holmdahl, R., L. Jansson, A. Larsson, and R. Jonsson. 1990. Arthritis in DBA/1 mice induced with passively transferred type II collagen immune serum. Immunohistopathology and serum levels of anti-type II collagen auto-antibodies. *Scand. J. Immunol.* 31:147–157. http://dx.doi.org/10.1111/j.1365-3083.1990.tb02754.x

Karlsson, R., J.A. Mo, and R. Holmdahl. 1995. Binding of autoreactive mouse anti-type II collagen antibodies derived from the primary and the secondary immune response investigated with the biosensor technique. *J. Immunol. Methods.* 188:63–71. http://dx.doi.org/10.1016/0022-1759(95)00203-0

Klaczkowska, D., B. Raposo, and K.S. Nandakumar. 2011. Heterogeneous stock mice are susceptible to encephalomyelitis and antibody-initiated arthritis but not to collagen- and G6PI-induced arthritis. *Scand. J. Immunol.* 73:46–52. http://dx.doi.org/10.1111/j.1365-3083.2010.02479.x

Laskowski, R.A., M.W. MacArthur, D.S. Moss, and J.M. Thornton. 1993. Procheck - a Program to Check the Stereochemical Quality of Protein Structures. *J. Appl. Cryst.* 26:283–291. http://dx.doi.org/10.1107/S0021889892009944

Leslie, A.G.W., and H.R. Powell. 2007. Processing diffraction data with MOSFLM. *In* Evolving Methods for Macromolecular Crystallography. R.J. Read and J.L. Sussman, editors. Springer. 41–52.

Luross, J.A., and N.A. Williams. 2001. The genetic and immunopathological processes underlying collagen-induced arthritis. *Immunology.* 103:407–416. http://dx.doi.org/10.1046/j.1365-2567.2001.01267.x

Mo, J.A., and R. Holmdahl. 1996. The B cell response to autologous type II collagen: biased V gene repertoire with V gene sharing and epitope shift. *J. Immunol.* 157:2440–2448.

Mullazehi, M., L. Mathsson, J. Lampa, and J. Rönnelid. 2007. High anti-collagen type-II antibody levels and induction of proinflammatory cytokines by anti-collagen antibody-containing immune complexes in vitro characterise a distinct rheumatoid arthritis phenotype associated with acute inflammation at the time of disease onset. *Ann. Rheum. Dis.* 66:537–541. http://dx.doi.org/10.1136/ard.2006.064782

Nandakumar, K.S., and R. Holmdahl. 2005. Efficient promotion of collagen antibody induced arthritis (CAIA) using four monoclonal antibodies specific for the major epitopes recognized in both collagen induced arthritis and rheumatoid arthritis. *J. Immunol. Methods.* 304:126–136. http://dx.doi.org/10.1016/j.jim.2005.06.017

Nandakumar, K.S., L. Svensson, and R. Holmdahl. 2003. Collagen type II-specific monoclonal antibody-induced arthritis in mice: description of the disease and the influence of age, sex, and genes. *Am. J. Pathol.* 163:1827–1837. http://dx.doi.org/10.1016/S0002-9440(10)63542-0

Nandakumar, K.S., A.K.B. Lindqvist, and R. Holmdahl. 2011. A dominant suppressive MHC class II haplotype interacting with autosomal genes controls autoantibody production and chronicity of arthritis. *Ann. Rheum. Dis.* 70:1664–1670. http://dx.doi.org/10.1136/ard.2011.151738

Olee, T., P.M. Yang, K.A. Siminovitch, N.J. Olsen, J. Hillson, J. Wu, F. Kozin, D.A. Carson, and P.P. Chen. 1991. Molecular basis of an autoantibody-associated restriction fragment length polymorphism that confers susceptibility to autoimmune diseases. *J. Clin. Invest.* 88:193–203. http://dx.doi.org/10.1172/JCI115277

Stuart, J.M., and F.J. Dixon. 1983. Serum transfer of collagen-induced arthritis in mice. *J. Exp. Med.* 158:378–392. http://dx.doi.org/10.1084/jem.158.2.378

Svensson, L., J. Jirholt, R. Holmdahl, and L. Jansson. 1998. B cell-deficient mice do not develop type II collagen-induced arthritis (CIA). *Clin. Exp. Immunol.* 111:521–526. http://dx.doi.org/10.1046/j.1365-2249.1998.00529.x

Vencovský, J., E. Zďárský, S.P. Moyes, A. Hajeer, S. Ruzicková, Z. Cimburek, W.E. Ollier, R.N. Maini, and R.A. Mageed. 2002. Polymorphism in the immunoglobulin VH gene V1-69 affects susceptibility to rheumatoid arthritis in subjects lacking the HLA-DRB1 shared epitope. *Rheumatology (Oxford).* 41:401–410. http://dx.doi.org/10.1093/rheumatology/41.4.401

Wooley, P.H., H.S. Luthra, J.M. Stuart, and C.S. David. 1981. Type II collagen-induced arthritis in mice. I. Major histocompatibility complex (I region) linkage and antibody correlates. *J. Exp. Med.* 154:688–700. http://dx.doi.org/10.1084/jem.154.3.688